# Stereochemistry of Glutamate Receptor Agonist Efficacy: Engineering a Dual-Specificity AMPA/Kainate Receptor†

Dean R. Madden,‡,§ Qing Cheng,|| Shalita Thiran,⊥ Shanti Rajan,|| Frank Rigo,⊥ Kari Keinänen,# Stefan Reinelt,§ Herbert Zimmermann,§ and Vasanthi Jayaraman*,||

*Department of Integrative Biology and Pharmacology, University of Texas Health Science Center, Houston, Texas 77030, Department of Biochemistry, Dartmouth Medical School, Hanover, New Hampshire 03755, Max Planck Institute for Medical Research, Heidelberg, Germany, Chemistry Department, Marquette University, Milwaukee, Wisconsin 53233, and Department of Biological and Environmental Sciences, University of Helsinki, Finland, FI-00014*

*Received July 21, 2004; Revised Manuscript Received October 6, 2004*

ABSTRACT: Upon agonist binding, the bilobate ligand-binding domains of the ionotropic glutamate receptors (iGluR) undergo a cleft closure whose magnitude correlates broadly with the efficacy of the agonist. AMPA (α-amino-5-methyl-3-hydroxy-4-isoxazolepropionic acid) and kainate are nonphysiological agonists that distinguish between subsets of iGluR. Kainate acts with low efficacy at AMPA receptors. Here we report that the structure-based mutation L651V converts the GluR4 AMPA receptor into a dual-specificity AMPA/kainate receptor fully activated by both agonists. To probe the stereochemical basis of partial agonism, we have also investigated the correlation between agonist efficacy and a series of vibrational and fluorescence spectroscopic signals of agonist binding to the corresponding wild-type and mutant GluR4 ligand-binding domains. Two signals track the extent of channel activation: the maximal change in intrinsic tryptophan fluorescence and the environment of the single non-disulfide bonded C426, which appears to probe the strength of interactions with the ligand α-amino group. Both of these signals arise from functional groups that are poised to detect changes in the extent of channel cleft closure and thus provide additional information about the coupling between conformational changes in the ligand-binding domain and activation of the intact receptor.

Most excitatory synaptic signals in the brain are carried by glutamate receptor ion channels (iGluR)[1] (*1*−*8*). As for most ligand-gated ion channels, activation is followed by desensitization in the continuing presence of agonist. The site of agonist binding is formed between two lobes of an extracellular ligand-binding domain known as S1S2. Crystallographic analysis of the S1S2 domain from the α-amino-5-methyl-3-hydroxy-4-isoxazolepropionic acid (AMPA)-specific iGluR subunit GluR2 has provided insights into the mechanism of agonist-induced activation and desensitization of this receptor (*1*−*5*, *9*−*12*). Binding of various agonists is observed to stabilize closed-cleft forms of the domain, with the degree of cleft closure approximately proportional to the efficacy of the agonist. The domains also dimerize back-to-back via the membrane-distal lobe. As a result, it has been proposed that S1S2 cleft closure provides the mechanism for receptor activation via increased separation of the transmembrane domains (*1*, *5*, *9*). Crystallographic analysis of the GluR2-S1S2 domain bound to the partial agonist kainate revealed that the side chain of L650 interacts with the kainate isopropenyl group, apparently preventing complete cleft closure via a "foot in the door" mechanism (*9*) The homologous L646T mutation in GluR1 affects the $EC_{50}$ value and desensitization properties of kainate (*13*), and the corresponding L650T mutation in GluR2 yields a subunit for which kainate efficacy is increased, but AMPA efficacy is decreased, such that both are partial agonists (*14*). In the latter case, parallel structural studies revealed that kainate induces a cleft closure in the L650T-S1S2 domain larger than in the WT domain, but still not as large as that induced by the full agonist glutamate, consistent with the observed efficacy change (*14*).

While rigid-body motions between the S1S2 lobes are clearly important predictors of channel activation, recent spectroscopic studies have revealed changes in the organization and dynamics of the ligand-binding domain that may also play a role in gating and desensitization processes. NMR studies, for instance, suggest that the S1S2 protein is not a rigid structure, and that lobe 2, which interacts with the γ-substituents of various agonists, exhibits considerable

† This work was supported by the American Heart Association of Texas and the National Science Foundation (NSF-0096635) (V.J.), the Academy of Finland (K.K.), the Max Planck Society (H.Z., D.R.M.), and the Deutsche Forschungsgemeinschaft and HHMI Biomedical Research Support Program to Medical Schools Award #76200-560801 (D.R.M.).

* To whom correspondence should be addressed. Mailing address: MSB 4.106, 6341 Fannin, Department of Integrative Biology and Pharmacology, University of Texas Health Science Center, Houston, TX 77030. Telephone: 713-500-6236. Fax: 713-500-7444. E-mail: vasanthi.jayaraman@uth.tmc.edu.

‡ Dartmouth Medical School.

§ Max Planck Institute for Medical Research.

|| University of Texas Health Science Center.

⊥ Marquette University.

# University of Helsinki.

[1] Abbreviations: ionotropic glutamate receptors, iGluR; α-amino-5-methyl-3-hydroxy-4-isoxazolepropionic acid, AMPA; cyclothiazide, CZ.

10.1021/bi048447y CCC: $27.50 
Published on Web 11/24/2004

mobility on the microsecond to millisecond time scale (*2*, *12*). Modeling studies suggest that agonist binding may stabilize the lobe (*15*). Since this region of the protein is directly connected to the transmembrane segments, its dynamic motions may well play a role in channel gating (*12*).

Stereochemical changes associated with agonist binding also have been characterized by our previous spectroscopic work with the full-length S1S2 domain of the AMPA receptor subunit GluR4. Using vibrational and fluorescence techniques, we have been able to identify a panel of signals that distinguish between the partial agonist kainate and the full agonist glutamate. Some of these signals reflect the stereochemical environment of the ligand, whereas others reflect the overall conformation of the domain (*16*−*18*).

L651 is the GluR4 side chain homologous to L650 in GluR2. Here we show that, unlike GluR2-L650T, the GluR4-L651V mutation converts kainate to a bona fide full agonist, equivalent to both glutamate and AMPA in its efficacy. To investigate the stereochemical basis of partial vs full agonism, we have compared the spectroscopic behavior of both wild-type and mutant ligand-binding domains in order to characterize which signals reliably distinguish between full and partial agonists and thus to probe which stereochemical interactions underpin channel activation.

## MATERIALS AND METHODS

*Electrophysiological Measurements.* Human embryonic kidney 293 (HEK293) cells (ATCC CRL 1573) were cultured in DMEM supplemented with 10% fetal bovine serum (Life Technologies, Bethesda, MD) and 2 mM glutamine, 50 $\mu$g/mL penicillin, and 50 $\mu$g/mL streptomycin. Transfections were performed using Fugene-6 (Roche, Indianapolis, In) transfection reagent, with 1−2 $\mu$g of glutamate receptor cDNAs and 0.5 $\mu$g of plasmid containing the cDNA for green fluorescent protein. The plasmid encoding the GluR4-flip subunit of the glutamate receptors used for the transfection was generously provided by Dr. Seeburg (Max Planck Institute, Heidelberg, Germany). The L651V point mutation was introduced in the plasmids using the Stratagene QuikChange XL site-directed mutagenesis kit (Stratagene, CA), and the integrity of the final construct verified by sequencing the coding region for both strands of the DNA.

Whole-cell measurements were performed on cells 2−3 days after transfection. The flow device used for the whole-cell measurements was a U-tube with a 100 $\mu$m aperture. Using a flow rate of 5 cm/s and a cell-aperture distance of 50 $\mu$m, the equilibration of the cell-surface receptors with the ligand solution occurs within tens of milliseconds. The time constant for ionic exchange as measured with an open-tip pipet was less than 10 ms.

For the electrophysiological measurements, the electrode solution contained 140 mM CsCl, 2 mM $MgCl_2$, 1 mM $CaCl_2$, 10 mM EGTA, 2 mM $Na_2ATP$, and 10 mM HEPES (pH 7.4); the extracellular bath solution contained 145 mM NaCl, 1.8 mM $MgCl_2$, 1 mM $CaCl_2$, 3 mM KCl, 10 mM glucose, and 10 mM HEPES (pH 7.4). Whole-cell currents were amplified with an Axon 200B amplifier and low-pass-filtered at 1 kHz for the whole-cell experiments, since the time resolution of the mixing device was 10 ms. The filtered signal was digitized using a Labmaster DMA digitizing board controlled by Axon PClamp software. All experiments were performed at room temperature, at pH 7.4, and at a membrane potential of −60 mV. Cyclothiazide (CZ) (100 $\mu$M) used for the whole-cell measurements was prepared in extracellular buffer from a 20 mM stock solution of cyclothiazide dissolved in DMSO. We have observed that complete block of desensitization requires preincubation. Hence, prior to recording currents in the presence of CZ, cells were preincubated with 100 $\mu$M cyclothiazide for a few minutes. Reference desensitizing currents were recorded on the same cells prior to the application of CZ.

*S1S2 Protein Preparation.* A transfer plasmid encoding the GluR4-S1S2-L651V mutant was generated from the wild-type sequence using PCR techniques and verified by DNA sequencing, and recombinant baculovirus was produced in the Bac-to-Bac system (Invitrogen) as described (*19*). Wild-type and mutant GluR4-S1S2 protein was expressed, purified, and characterized as described (*18*). In brief, S1S2 proteins were expressed as secreted constructs in the baculovirus system. Following clarification and concentration of cell-culture supernatants, they were purified to homogeneity by immunoaffinity and ion-exchange chromatography.

*Synthesis of Isotopically Labeled AMPA.* The key intermediate 4-(bromomethyl)-2-(methoxymethyl)-5-methylisoxalin-3-one (**I**) was obtained by bromomethylation of 3-hydroxy-5-methylisoxalole (Tachigaren) (*20*, *21*) with 1,3,5-trioxane in 62% hydrobromic acid, followed by conversion of the 2-bromomethyl group to 2-methoxymethyl in $CH_2Cl_2$ with methanol. 1,3-$^{13}C_2$-Dimethyl malonate was reacted with sodium nitrite, followed by reductive acylation with zinc and acetanhydride to yield 1,3-$^{13}C_2$-dimethyl acetamidomalonate. The ion of this compound was prepared with sodium hydride in DMF and reacted with **I** to yield methyl 2-acetamido-2-methoxy-$^{13}$C-carbonyl-3-(2-(methoxymethyl)-5-methyl-3-oxoisoxalin-4-yl)-1-$^{13}$C-propanoate. Refluxing in 1 molar trifluoroacetic acid yielded α-$^{13}$COOH-labeled (*RS*)-AMPA (*22*, *23*). All labeled and unlabeled intermediates were checked by mass spectrometry, $^1$H NMR, and TLC. The products were checked by $^1$H and $^{13}$C NMR, which confirmed labeling at the expected site with chemical purity better than 99%.

*FTIR Difference Spectroscopy.* Protein (0.25−0.5 mM) in 25 mM phosphate buffer containing 250 mM NaCl and 0.02% $NaN_3$ was used for the FTIR measurements. $D_2O$ was used as the solvent to obtain the spectra in the 1450−1800 $cm^{-1}$ region, since water has a large infrared absorption band at ∼1600 $cm^{-1}$. However, for studying the S-H stretching vibration, water was used as the solvent.

The FTIR spectra were obtained using a Nicolet Nexus 870. A modified variable-length sample holder (Aldrich, Milwaukee, WI) with $CaF_2$ windows was used to obtain the spectra. Spectra were collected at 4 $cm^{-1}$ spectral resolution, and at a constant temperature of 15 °C. A 50-$\mu$m path length was used to obtain the spectra in the 1450−1800 $cm^{-1}$ region, and a 75-$\mu$m path length was used for studying the S−H vibration. The difference spectra were generated by subtracting the spectra of the unligated form of the protein from the ligated form of the protein. The subtraction was performed using as an internal standard the band at 2045 $cm^{-1}$ arising from the sodium azide present in the buffer. Furthermore, the peaks that arise from the unbound agonists were subtracted using a spectrum of the agonist in $D_2O$.

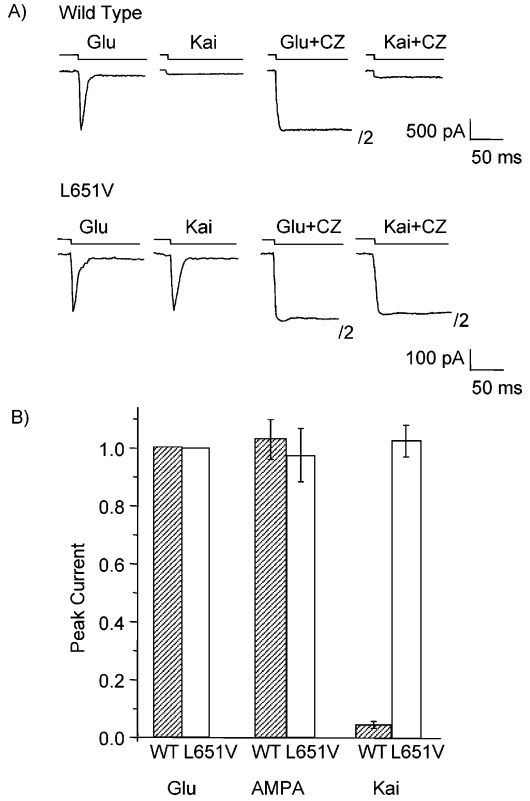


FIGURE 1: (A) Whole-cell currents evoked from HEK-293 cells transiently transfected with the plasmid for wild-type or L651V GluR4-flip receptor subunits due to application of 10 mM glutamate (Glu) and 10 mM kainate (Kai) in the absence and presence of 100 mM cyclothiazide (+CZ). The duration for which the ligand solution was applied is shown above each current trace. The nondesensitizing currents due to activation of wild-type channels by Glu+CZ as well of L651V channels by Glu+CZ or Kai+CZ are divided by two ("/2") for scaling purposes. (B) Bar graph showing peak nondesensitizing currents for the wild-type and L651V mutant receptors during application of 10 mM glutamate, 10 mM AMPA, or 10 mM kainate, normalized to the glutamate currents, all in the presence of 100 $\mu$M cyclothiazide. Data represent averages from at least six measurements for each ligand, obtained from four cells.

*Fluorescence Spectroscopy.* Fluorescence titrations were performed essentially as described (*18*). To obtain a robust estimate of the maximal intrinsic fluorescence change, the protein was used at concentrations of 100−200 nM in 10 mM sodium phosphate, pH 7.3. Following each addition of ligand, the sample was allowed to equilibrate for 30 s before measurement. The values of the equilibrium dissociation constant ($K_d$) and the maximum fluorescence change ($\Delta F_{max}$) were obtained by fitting a single-site binding equation to the data (*18*). For measurements with kainate, an additional linear absorption factor was included in the model to compensate for the inner-filter effect of kainate absorbance ($OD_{em} + OD_{ex} \leq 0.1$). Each result represents the average of at least two independent titrations.

## RESULTS AND DISCUSSION

*Kainate Is a Full Agonist for GluR4-L651V.* Representative whole-cell currents are shown for the wild-type and L651V mutant homomeric GluR4 receptors in Figure 1A. Desensitizing currents were measured in the presence of saturating concentrations of glutamate (10 mM) and kainate (10 mM). To assess the extent of activation, the receptor responses have also been characterized in the presence of cyclothiazide, and representative data for glutamate and kainate are shown in Figure 1A (right-hand traces). The magnitude of the average nondesensitizing peak currents is compared for mutant and wild-type receptors in Figure 1B. As expected, cells expressing wild-type GluR4 receptors exhibit much smaller activation and reduced desensitization in response to saturating concentrations of the partial agonist kainate compared to the full agonists. In contrast, the kainate response of cells expressing GluR4-L651V receptors was indistinguishable in magnitude or extent of desensitization (based on the residual current at longer times in the continued presence of agonist) from the responses induced by full agonists (Figure 1 and Table 1). Additionally, the rate of desensitization following activation of GluR4-L651V by 10 mM kainate (7.2 ± 2 ms) was similar to those observed for GluR4-L651V (6.8 ± 2 ms) and wild-type GluR4 (7.1 ± 2 ms) following activation by 10 mM glutamate. These results suggest that the L651V mutant converts kainate from a partial to a full agonist of GluR4 channels, providing the first example of a completely bispecific AMPA/kainate iGluR.

Table 1: Relative Agonist Efficacy[a]

| | GluR4-WT | GluR4-L651V | GluR2-WT[b] | GluR2-L650T[b] |
|---|---|---|---|---|
| glutamate | 1.0 | 1.0 | 1.0 | 1.0 |
| AMPA | 1.03 | 0.98 | 1.16 | 0.31 |
| kainate | 0.05 | 1.03 | 0.17 | 0.45 |

[a] Agonist efficacy calculated as the ratio between the maximal current response to a given agonist and that to glutamate, in the presence of cyclothiazide. [b] For comparison, values are included for GluR2 and GluR2-L650T (*14*).

These results are consistent with earlier predictions based on affinity and desensitization measurements with the GluR1 subunit (*13*) and on the stereochemistry of the kainate:S1S2 binding interaction (*9*). However, somewhat different electrophysiological behavior has recently been reported for the corresponding L650T mutant in the GluR2 background. Like GluR4-L651V, this mutation increases the kainate:glutamate response ratio. Unlike GluR4-L651V, in GluR2-L650T, the kainate response remains significantly smaller than the glutamate response, and AMPA is converted from a full to a partial agonist (*14*). Since Val and Thr are isosteric, the different pharmacological responses of GluR4-L651V and GluR2-L650T to kainate and AMPA cannot be explained by purely steric ("foot-in-the-door") restrictions on the extent of cleft closure, but rather must depend on the detailed stereochemistry of the interaction or perhaps on the differential behavior of homomeric GluR2 and GluR4 channels.

*Spectroscopic Differences between Partial and Full Agonist-Bound Forms of S1S2.* Most crystal structures of the GluR2-S1S2 protein indicate that the degree of domain closure correlates with the extent of activation of the channel. Several spectroscopic signals have also been identified that can be used to monitor the ligand-binding process and provide information on distinct stereochemical components of the binding (*16*−*18*). To identify which of these component interactions contribute to agonist efficacy, we have compared the associated spectroscopic signals for a series of agonist complexes with both WT and L651V-S1S2 domains of GluR4. The signals reflect changes in S1S2 secondary structure content and in the environments of the

Table 2: Asymmetric Carboxylate Vibrations of the Agonist α-Carboxylates

| ligand | $\nu_{asym\alpha}$ ($cm^{-1}$) free | $\nu_{asym\alpha}$ ($cm^{-1}$) S1S2 bound | $\Delta G_{binding}$ (kcal/mol) |
|---|---|---|---|
| | WT | | |
| kainate | 1620 | 1605 | −5.0 |
| glutamate | 1614 | 1610 | −1.3 |
| AMPA | 1614 | 1605 | −3.0 |
| | L651V | | |
| kainate | 1620 | 1605 | −5.0 |
| glutamate | 1614 | 1608 | −2.0 |

ligand α-carboxylate group, the single free S1S2 thiol group, and the S1S2 tryptophan residues distant from the binding site.

*The α-Carboxylate Binding Environment.* The asymmetric carboxylate stretching vibration is a sensitive monitor of the overall electrostatic environment of the group and varies linearly with the strength of the noncovalent interactions: a 3 $cm^{-1}$ downshift corresponds approximately to a −1 kcal/mol change in enthalpy at the carboxylate (*24*). To probe the environments of the α-carboxylate moiety conserved among the partial agonist kainate and the full agonists glutamate and AMPA, we compared the band shifts upon binding to S1S2. The band shifts for glutamate and kainate upon binding to the S1S2 domain have been previously reported (*16*). Upon S1S2 binding, the asymmetric α-carboxylate modes of glutamate and kainate exhibit downshifts of 4 and 15 $cm^{-1}$, corresponding to favorable $\Delta G_{binding}$ values of −1.3 and −5.0 kcal/mol, respectively (*24*) (Table 2).

Here we have investigated the environment of the α-carboxylate moiety of AMPA in S1S2 by obtaining difference FTIR spectra between free AMPA and $D_2O$, and between the S1S2:AMPA complex and free S1S2 protein (Figure 2, traces A and C). Features are observed at 1659 and 1614 $cm^{-1}$. To assign the AMPA α-carboxylate vibrations, $^{13}C$-α-AMPA was synthesized, and difference spectra were obtained between the labeled and unlabeled compound for both the free and bound states of AMPA (Figure 2, traces B and D). On the basis of the difference spectrum obtained with the isotopically labeled AMPA, the frequency of the α-carboxylate vibration of AMPA in the free state is 1614 $cm^{-1}$ and is downshifted to 1605 $cm^{-1}$ when bound to S1S2 (Table 2). The 1659 $cm^{-1}$ band has been tentatively assigned to the AMPA isoxazole moiety. The 9 $cm^{-1}$ shift in α-carboxylate frequency corresponds to a $\Delta G_{binding}$ of −3.0 kcal/mol, which is significantly more favorable than the −1.3 kcal/mol observed for glutamate but smaller than the −5.0 kcal/mol observed for kainate. Similar results have been found for the GluR2-S1S2 domain (*25*).

The analysis was extended to include kainate and glutamate binding to the GluR4-S1S2-L651V mutant domain (Figure 3, traces D and E). The α-carboxylate vibrational modes of the kainate:L651V and glutamate:L651V complexes are at frequencies similar to those observed with the wild-type complexes. This indicates that the mutation has only a minor effect on the stereochemical interactions of the α-carboxylate moiety within the binding pocket.

The observation of favorable interactions between the α-carboxylate moiety and the S1S2 protein is consistent with the crystal structures of GluR2-S1S2 in complex with glutamate, AMPA, and kainate (*9*), all of which reveal an essentially identical interaction between the ligand carboxylate and a binding site that contains a positively charged arginine side chain (R486; residue numbering is based on mature GluR4 full-length protein). However, as described above, the spectroscopic analysis of the α-COOH binding interaction suggests subtle differences in the energetics of these interactions. The S1S2-induced downshifts in the $\nu_{asym\alpha}$ mode, and thus the strength of their binding interactions, apparently follow the order kainate > AMPA > glutamate, with a difference in free energy change of −3.7 kcal/mol between the strongest (kainate) and weakest (glutamate) interactions.

This suggests that, at least in the solution state, the α-COOH substituents of the agonists may undergo slight adjustments in their docking against lobe 1, which could play

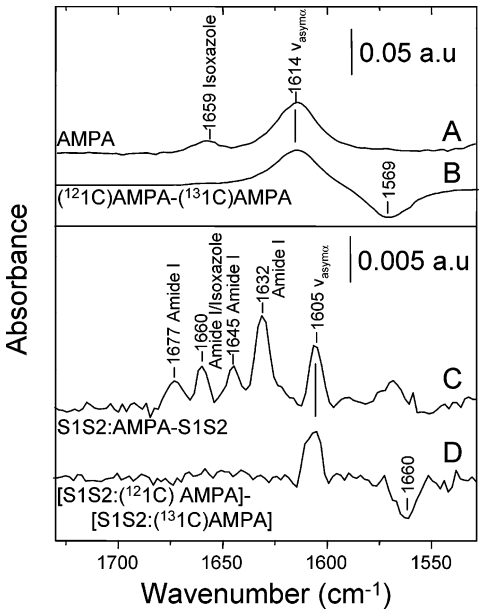


FIGURE 2: Difference FTIR spectrum between (A) AMPA and $D_2O$ (AMPA), (B) $^{12}C$-α-AMPA and $^{13}C$-α-AMPA, (C) AMPA-bound (S1S2:AMPA) and unligated form of GluR4-S1S2 protein, and (D) $^{12}C$-α-AMPA-bound GluR4-S1S2 and $^{13}C$-α-AMPA-bound GluR4-S1S2.

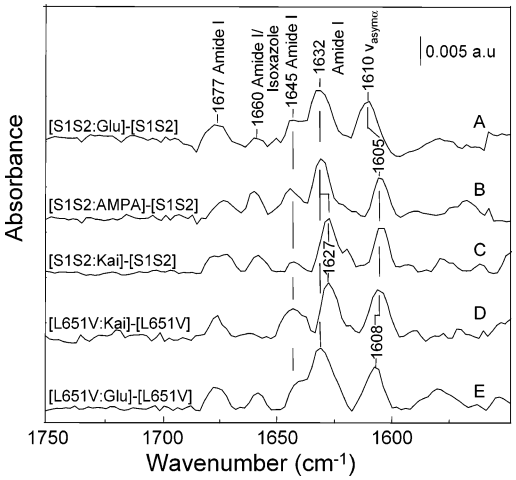


FIGURE 3: Difference FTIR spectrum between (A) glutamate-bound and unligated form of GluR4-S1S2 protein in $D_2O$, (B) AMPA-bound and unligated form of GluR4-S1S2 protein in $D_2O$, (C) kainate-bound and unligated form of GluR4-S1S2 protein in $D_2O$, (D) kainate-bound and unligated form of L651V-S1S2 protein in $D_2O$, and (E) glutamate-bound and unligated form of L651V-S1S2 protein in $D_2O$.

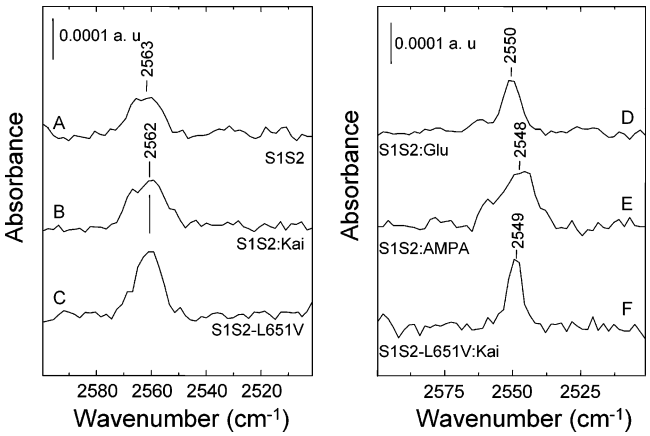


FIGURE 4: FTIR spectra in $H_2O$ of (A) unligated form of S1S2, (B) kainate-bound form of S1S2, (C) unligated form of L651V-S1S2, (D) glutamate-bound form of S1S2, (E) AMPA-bound form of S1S2, and (F) kainate-bound form of L651V-S1S2.

a role in net affinity differences and potentially even in the function associated with these agonists. However, the strength of the noncovalent interactions at the α-carboxylate (kainate > AMPA > glutamate) does not track the extent of channel activation (AMPA ≈ glutamate > kainate). Furthermore, since the strength of the noncovalent interactions at this residue for the ligand kainate is unaffected by the L651V mutation, which converts kainate from a partial to a full agonist, it evidently does not reflect interactions that track efficacy. This is consistent with the proposal that distinct steps mediate ligand binding and channel activation. Agonists dock first to lobe 1, primarily with their α substituents, in a relatively conserved orientation. Channel activation is then triggered by subsequent cleft closure, which involves interactions between lobe 2 and the ligand's α-amino and γ-substituents. Mutations in lobe 2, such as L651V, should affect primarily the second step ("locking"), but not the first ("docking") (*18*).

*Cysteine 426 and the α-Amino Binding Interaction.* The SH stretching vibration of the single non-disulfide bonded cysteine (C426) in the GluR4-S1S2 protein was monitored for the unligated form and for the kainate-, glutamate-, and AMPA-bound forms in $H_2O$ (Figure 4). The stretching mode occurs in a region that is well-separated from the vibrational bands of other protein moieties. It is also extremely sensitive to even slight changes in hydrogen-bond strength, with a ∼18 $cm^{-1}$ shift in the SH vibrational frequency correlated to a change in distance of the SH bond by 0.1 Å (*26*). As a result, it is an excellent probe for studying the noncovalent interactions at the C426 residue. As for the GluR2-S1S2 domain (*25*), the frequency of the SH stretching band at 2563 $cm^{-1}$ in the unligated state of wild-type and 2562 $cm^{-1}$ in the L651V mutant domains (Figure 4, traces A and C) indicates that the SH group forms a medium-strength hydrogen bond in both wild-type and L651V mutant GluR4-S1S2 domains. On the basis of the GluR2 crystal structure (*9*), possible hydrogen-bond acceptor atoms include the carbonyl oxygen atoms of Ala 478 or Ile 477, both at a distance of ∼4 Å from the cysteine sulfur atom. This is somewhat further than the distance suggested by the vibrational frequency. However, thiol hydrogen bonds are typically ∼3.5 Å in length (*27*), so that only relatively small adjustments would be required.

Furthermore, the C426 SH stretching frequency is not significantly altered upon kainate binding to wild-type S1S2 (Figure 4, trace B), indicating that the environment of this cysteine residue is not significantly altered in the presence of the ligand kainate. On the other hand, the frequency of this mode is lowered to 2550 and 2548 $cm^{-1}$, respectively, upon binding glutamate (Figure 4, trace D) and AMPA (Figure 4, trace E). Additionally, the SH stretching frequency for the kainate-bound form of the L651V mutant indicated a downshift to 2549 $cm^{-1}$ (Figure 4, trace F), similar to that observed for the glutamate- and AMPA-bound forms of the wild-type protein. The downshift of ∼15 $cm^{-1}$ upon full agonist binding corresponds to a strengthening of the SH hydrogen bond relative to the unligated and partial agonist bound forms.

The different effects of full and partial agonists on C426 (full agonist > partial agonist ≈ apo) do appear to provide a good binary indicator of full agonism, since they clearly distinguish kainate from AMPA and glutamate in the wild-type domain and since the kainate signal shifts in the presence of the L651V mutation to match that of the full agonists. Furthermore, although the changes do not correlate with the degree of domain closure observed for the various agonists in the GluR2 X-ray structures (full agonist > partial agonist > apo), they do correspond approximately to the relative efficacy (full agonist > partial agonist ≈> apo) (Table 1 and ref *14*).

It is likely that the changes at the C426 residue reflect the strength of the interactions of the ligand α-amino group with the protein, since P479, which is hydrogen bonded to the amine groups of the ligands, is adjacent to the candidate hydrogen-bonding partners of C426 (I477 and A478). The α-amino group also mediates a three-way hydrogen-bonding network with E706 and T481 (*28*). This tripartite interaction knits both lobes of the domain together with the agonist during the "locking" step and may be important for channel activation (*18*). As a result of its interaction with side chains on both sides of the binding cleft, the α-amino group is well-positioned to monitor differences in lobe closure associated with the binding of different agonists. In addition, as noted for the α-carboxylate moiety, it is possible that stereochemical accommodation of different γ-substituents may require subtle adjustments of the binding geometry of the α-amino group. This could, in turn, affect the tripartite hydrogen-bond interaction and thus exert a secondary influence on the extent of cleft closure.

*Secondary Structure.* Another vibrational spectroscopy signal involves secondary structural changes triggered by agonist binding. Features are seen at 1677, 1660, 1645, and 1632 $cm^{-1}$ in the difference spectrum between the glutamate-bound and unligated forms of the wild-type S1S2 domain (Figure 3, trace A). They can be assigned to the amide I modes arising from the protein backbone, since no side chains are expected to have vibrational modes in this region in $D_2O$. The 1677 and 1632 $cm^{-1}$ bands have been assigned to changes in turns and β-sheet structures, respectively (*29*). The exact nature of the secondary structural change cannot be clearly determined for the 1660 and 1645 $cm^{-1}$ bands, since amide I vibrations at these frequencies can arise from multiple secondary structure elements (*30*, *31*). The positive bands at these frequencies with no corresponding negative features suggest that there is no significant change in content,

Table 3: Fluorescence Titration of Agonist Binding to S1S2

| ligand | $K_d$ ($\mu$M) | $\Delta F_{max}$ (% change) | GluR2 cleft closure[b] (deg) |
|---|---|---|---|
| | WT-S1S2 | | |
| kainate | $1.45 \pm 0.08$[a] | $-11 \pm 4$[a] | 12[b] |
| glutamate | $0.55 \pm 0.03$[a] | $-19 \pm 1$[a] | 20[b] |
| | L651V-S1S2 | | |
| kainate | $4.5 \pm 0.6$ | $-16.1 \pm 0.7$ | |
| glutamate | $1.3 \pm 0.1$ | $-23 \pm 1$ | |

[a] Ref *18*. [b] Ref *9*.

such as random coil to α-helices, but most likely arise due to changes in the dynamics of these secondary structures, consistent with reports that agonist binding may induce stabilization of lobe 2 (*12*, *15*).

Despite the overall similarities among the difference spectra associated with different agonists (Figure 3, traces A−C), there are three signals that distinguish among the various ligands. The increase in the $\beta$-sheet content is approximately the same for all the three ligands, but the frequency of the amide I band for the $\beta$-sheet changes is lower in the kainate-bound form (1627 $cm^{-1}$) than in the glutamate- and AMPA-bound (1632 $cm^{-1}$) forms. Additionally, the increase in the 1645 $cm^{-1}$ band is smaller for the kainate-bound form relative to the glutamate- and AMPA-bound forms (Figure 3, traces A−C). Finally, although there is only a slight difference in the wild-type 1660 $cm^{-1}$ bands in the presence of glutamate or kainate, changes are seen in L651V mutant spectra (see below). In the AMPA complex, this signal overlaps with the putative isoxazole of AMPA (Figure 2A) and thus cannot be readily interpreted.

To correlate the changes in secondary structure to differences in agonist efficacy, we have investigated kainate and glutamate activation of the L651V mutant (Figure 3, traces D and E). The difference spectrum for glutamate bound to L651V is similar to that of the wild-type S1S2 protein, suggesting that the mutation does not perturb the activation by glutamate (Figure 3, traces A and E). The intensity of the 1645 $cm^{-1}$ difference feature for L651V-S1S2 in the presence and absence of kainate is similar to that observed for the glutamate:WT and AMPA:WT complexes (Figure 3, traces A, B, and D) and different from that observed for the kainate:WT complex (Figure 3, trace C). However, the frequency of the amide I band for the $\beta$-sheet change in the kainate:L651V complex (1627 $cm^{-1}$) is identical to that observed in the kainate:WT complex. These results suggest that the differences in the 1645 $cm^{-1}$ band may be a signature for partial versus full agonism. In contrast, the shift in the frequency of the amide I band for the $\beta$-sheet between kainate and glutamate/AMPA appears to be ligand specific. As the magnitude of the 1660 $cm^{-1}$ mode differs more strongly between glutamate- and kainate-bound forms of L651V-S1S2 than for the wild type, in contradistinction to the electrophysiological data, it also does not appear to be a useful indicator of agonist efficacy.

*Fluorescence Spectroscopy.* Titration measurements using intrinsic fluorescence changes reveal that the affinity of the L651V-S1S2 mutant for kainate is weakened approximately 3-fold relative to wild-type, from 1.45 to 4.5 $\mu$M (Table 3). Thus, although the steric constraint to cleft closure provided by L651 has been reduced in volume, the overall free energy change of binding has become less favorable. This means that the contact of L651 with kainate must provide a favorable free energy of binding that is not entirely replaced by valine, even in conjunction with associated conformational rearrangements.

It had previously been observed that saturating concentrations of kainate induce a significantly smaller change in the intrinsic fluorescence of S1S2 ($\Delta F_{max}$) than do saturating concentrations of glutamate (*18*). The change in intrinsic S1S2 fluorescence upon agonist binding is mediated by tryptophan residues, and its relative magnitude tracks the degree of cleft closure detected crystallographically GluR2-S1S2 (Table 3). As no tryptophan residues are located in the ligand-binding cleft, the signal is likely to reflect overall conformational changes that result in distant side-chain environmental shifts. Candidate residues include a pair of adjacent tryptophan side chains (W767 and W768) located on the back face of the molecule near the hinge and essential for the stability and function of the domain (*12*). In particular, following superposition of lobe 1 of the GluR2-S1S2 core (*9*), the tryptophan corresponding to W768 is within 5 Å of several side chains whose relative positions shift in a graded fashion from the apo to the kainate- and AMPA-bound structures. No equivalent changes were detected in the environment of the other tryptophan side chains in the domain (W462 or W672). Thus, it appears likely that the maximal fluorescence changed may be mediated by and act as a good surrogate for the extent of cleft closure.

The magnitude of the intrinsic fluorescence change upon kainate binding is greater for the L651V mutant than for the wild-type GluR4 domain both in absolute terms (−16.1 vs −10.8%) and as a fraction of the change induced by glutamate binding (70 vs 57%) (Table 3). It thus appears that the L651V mutant reduces the steric clash with bound kainate, permitting a greater degree of cleft closure than in the wild-type. However, although the greater fluorescence change for the L651V mutant correlates qualitatively with the greater efficacy of kainate acting on GluR4-L651V channels, it does not quantitatively follow the conversion of kainate to a true full agonist, since the kainate fluorescence signal remains significantly smaller than that of glutamate. While it is possible that this discrepancy reflects a breakdown in the correlation between intrinsic fluorescence change and degree of cleft closure, the kainate:glutamate ratios for GluR4-S1S2 closely track the extent of cleft closure seen crystallographically for the isosteric GluR2-L650T mutant (70%; ∼15°) and GluR2-WT (57%; ∼12°), suggesting that $\Delta F_{max}$ may indeed act as a readout of cleft closure.

If so, it appears that L651V may only permit incomplete cleft closure upon kainate binding, as does the isosteric GluR2-L650T mutant (*14*). Alternatively, kainate may stabilize both partially and fully closed clefts, as is seen in crystal structures of AMPA bound to the GluR2-L650T-S1S2 domain (*14*). The increased relative fluorescence signal could then represent a shift in the equilibrium toward the fully closed state. However, regardless of the mechanistic interpretation, the kainate-induced fluorescence change is incomplete compared to that induced by glutamate, despite the fact that kainate is a full agonist for GluR4-L651V (Table 1). This could mean that the magnitude of S1S2 cleft closure seen for glutamate and AMPA may not be strictly required

for full agonism within the structural environment of the fully assembled channel but that smaller cleft closures might suffice, a hypothesis that can be tested by further crystallographic analysis.

## ACKNOWLEDGMENT

We thank U. Reygers for excellent technical assistance and the Biophysics Department (MPIMF) for use of the spectrofluorometer.

## REFERENCES

1. Mayer, M. L., and Armstrong, N. (2004) Structure and function of glutamate receptor ion channels, *Annu. Rev. Physiol. 66*, 161−81.
2. McFeeters, R. L., and Oswald, R. E. (2004) Emerging structural explanations of ionotropic glutamate receptor function, *Faseb J. 18*, 428−38.
3. Gouaux, E. (2004) Structure and function of AMPA receptors, *J. Physiol. 554*, 249−53.
4. Madden, D. R. (2002) The inner workings of the AMPA receptors, *Curr. Opin Drug Discovery Dev. 5*, 741−8.
5. Madden, D. R. (2002) The structure and function of glutamate receptor ion channels, *Nat. Rev. Neurosci. 3*, 91−101.
6. Dingledine, R., Borges, K., Bowie, D., and Traynelis, S. F. (1999) The glutamate receptor ion channels, *Pharm. Rev. 51*, 7−61.
7. Nakanishi, S., and Masu, M. (1994) Molecular diversity and functions of glutamate receptors, *Annu. Rev. Biophys. Biomol. Struct. 23*, 329−348.
8. Hollmann, M., and Heinemann, S. (1994) Cloned glutamate receptors, *Annu. Rev. Neurosci. 17*, 31−108.
9. Armstrong, N. A., and Gouaux, E. (2000) Mechanisms for activation and antagonism of an AMPA-sensitive glutamate receptor: Crystal structures of the GluR2 ligand binding core, *Neuron 28*, 165−181.
10. Hogner, A., Kastrup, J. S., Jin, R., Liljefors, T., Mayer, M. L., Egebjerg, J., Larsen, I. K., and Gouaux, E. (2002) Structural basis for AMPA receptor activation and ligand selectivity: Crystal structures of five agonist complexes with the GluR2 ligand-binding core, *J. Mol. Biol. 322*, 93−109.
11. Jin, R., Banke, T. G., Mayer, M. L., Traynelis, S. F., and Gouaux, E. (2003) Structural basis for partial agonist action at ionotropic glutamate receptors, *Nat. Neurosci. 6*, 803−10.
12. McFeeters, R. L., and Oswald, R. E. (2002) Structural mobility of the extracellular ligand-binding core of an ionotropic glutamate receptor. Analysis of NMR relaxation dynamics, *Biochemistry 41*, 10472−81.
13. Mano, I., Lamed, Y., and Teichberg, V. I. (1996) A venus flytrap mechanism for activation and desensitization of alpha-amino-3-hydroxy-5-methyl-4-isoxazole propionic acid receptors, *J. Biol. Chem. 271*, 15299−302.
14. Armstrong, N., Mayer, M., and Gouaux, E. (2003) Tuning activation of the AMPA-sensitive GluR2 ion channel by genetic adjustment of agonist-induced conformational changes, *Proc. Natl. Acad. Sci. U.S.A. 100*, 5736−41.
15. Arinaminpathy, Y., Sansom, M. S., and Biggin, P. C. (2002) Molecular dynamics simulations of the ligand-binding domain of the ionotropic glutamate receptor GluR2, *Biophys. J. 82*, 676−83.
16. Jayaraman, V., Keesey, R., and Madden, D. R. (2000) Ligand-protein interactions in the glutamate receptor, *Biochemistry 39*, 8693−8697.
17. Madden, D. R., Thiran, S., Zimmermann, H., Romm, J., and Jayaraman, V. (2001) Stereochemistry of quinoxaline antagonist binding to a glutamate receptor investigated by Fourier transform infrared spectroscopy, *J. Biol. Chem. 276*, 37821−37826.
18. Abele, R., Keinänen, K., and Madden, D. R. (2000) Agonist-induced isomerization in a glutamate receptor ligand-binding domain: A kinetic and mutagenetic analysis, *J. Biol. Chem. 275*, 21355−21363.
19. Lampinen, M., Pentikäinen, O., Johnson, M. S., and Keinänen, K. (1998) AMPA receptors and bacterial periplasmic amino acid-binding proteins share the ionic mechanism of ligand recognition, *EMBO J. 17*, 4704−4711.
20. Jacobsen, N., Kolind-Andersen, H., and Christensen, J. (1984) Synthesis of 3-isoxazolols revisited: Diketene and beta ketoesters as starting materials, *Can. J. Chem. 62*, 1940−1944.
21. Sørensen, U. S., Falch, E., and Krogsgaard-Larsen, P. (2000) A novel route to 5-substituted 3-isoxazolols. Cyclization of *N*,*O*-DiBoc $\beta$-keto hydroxamic acids synthesized via acyl Meldrum's acids, *J. Org. Chem. 65*, 1003−1007.
22. Honore, T., and Lauridsen, J. (1980) Structural analogues of ibotenic acid. Syntheses of 4-methyl-homoibotenic acid and AMPA, including the crystal structure of AMPA, monohydrate, *Acta. Chem. Scand. 34* (4B), 235−240.
23. Begtrup, M., and Sløk, F. A. (1993) Equilibrium control in bromomethylation: An expedient route to 2-amino-3-(3-hydroxy-5-methylisoxazol-4-yl)propionic acid (AMPA), *Synthesis 1993*, 861−863.
24. Cheng, Q., Thiran, S., Yernool, D., Gouaux, E., and Jayaraman, V. (2002) A vibrational spectroscopic investigation of interactions of agonists with GluR0, a prokaryotic glutamate receptor, *Biochemistry 41*, 1602−8.
25. Cheng, Q., and Jayaraman, V. (2004) Chemistry and conformation of the ligand-binding domain of GluR2 subtype of glutamate receptors, *J. Biol. Chem. 279*, 26346−50.
26. Li, H. M., and Thomas, G. J. (1991) Cysteine Conformation and Sulfhydryl Interactions in Proteins and Viruses. 1. Correlation of the Raman S−H Band with Hydrogen-Bonding and Intramolecular Geometry in Model Compounds, *J. Am. Chem. Soc. 113*, 456−462.
27. Ippolito, J. A., Alexander, R. S., and Christianson, D. W. (1990) Hydrogen bond stereochemistry in protein structure and function, *J. Mol. Biol. 215*, 457−471.
28. Armstrong, N., Sun, Y., Chen, G. Q., and Gouaux, E. (1998) Structure of a glutamate receptor ligand-binding core in complex with kainate, *Nature 395*, 913−7.
29. Spiro, T. G. (1987) *Biological applications of Raman spectroscopy*, Wiley, New York.
30. Byler, D. M., and Susi, H. (1986) Examination of the secondary structure of proteins by deconvolved FTIR spectra, *Biopolymers 25*, 469−487.
31. Chapman, D., Jackson, M., and Haris, P. I. (1989) Investigation of Membrane-Protein Structure Using Fourier Transform Infrared-Spectroscopy, *Biochem. Soc. Trans. 17*, 617−619.

BI048447Y